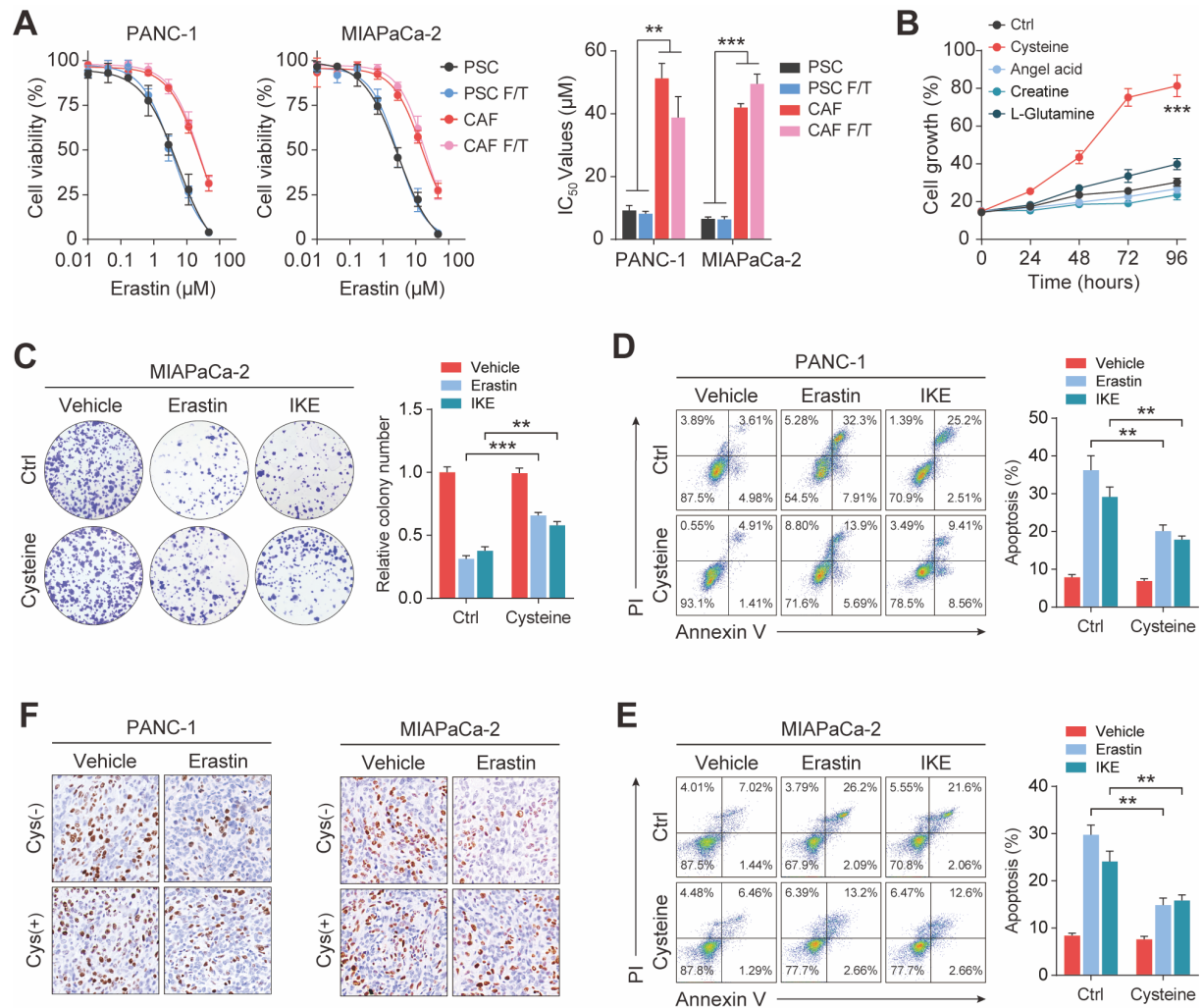


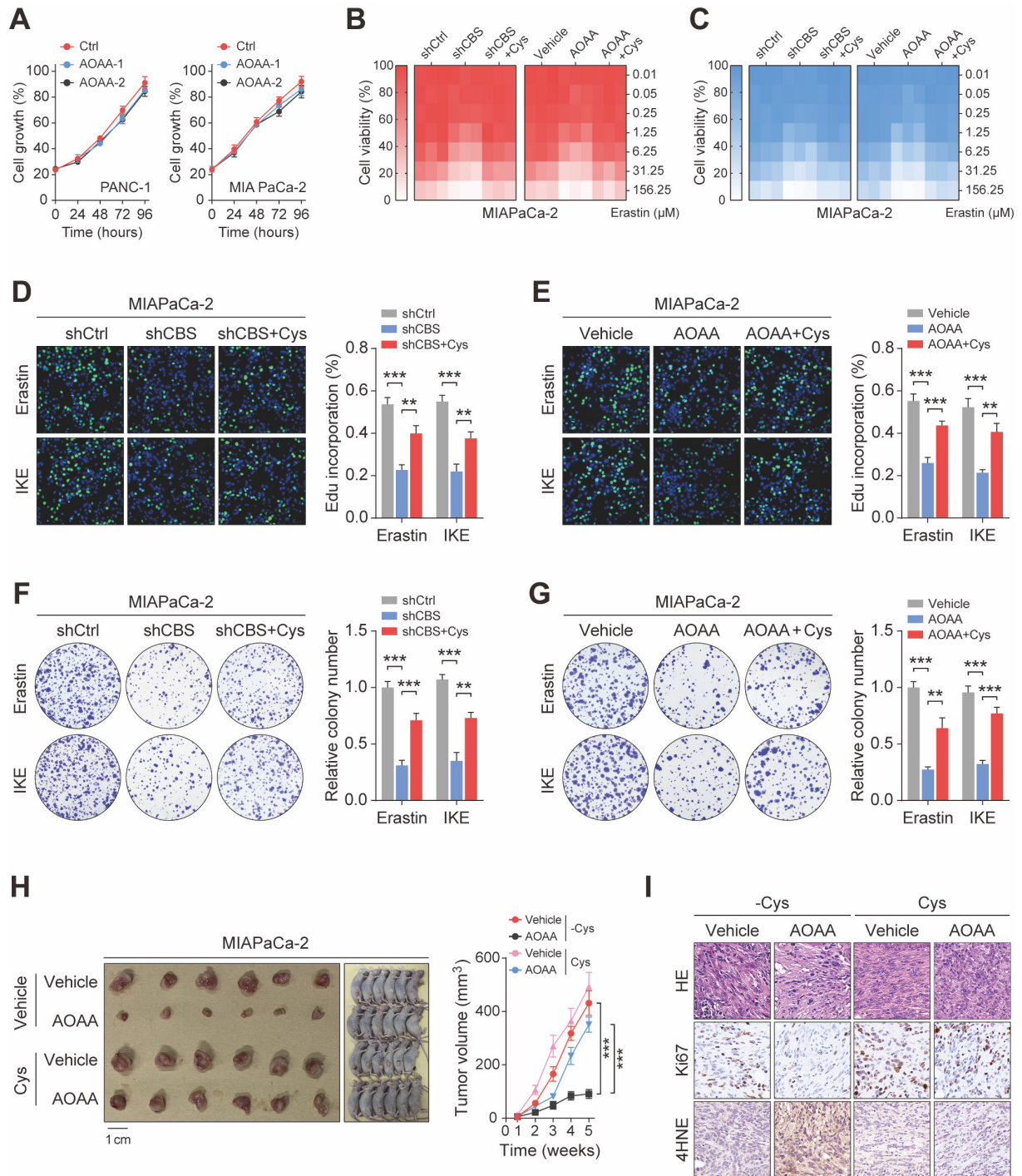
1  
2 **Figure S1. CAFs are associated with ferroptosis resistance in PDAC.** PDAC cells were  
3 cultured with CAF-CM or PCS-CM, and after (A-B) Erastin, RSL3, or IKE treatment, CCK-8  
4 was used to measure cell viability. (C-D) Colony formation by PANC-1 and MIAPaCa-2 cells  
5 was evaluated by clonal formation assay after treatment with vehicle, RSL3, or IKE. (E-F) Cell  
6 death ratios in PANC-1 and MIAPaCa-2 cells were evaluated by cell death assays after  
7 treatment with vehicle, RSL3, or IKE. \*  $P < 0.05$ , \*\*  $P < 0.01$ , \*\*\*  $P < 0.001$ .



8

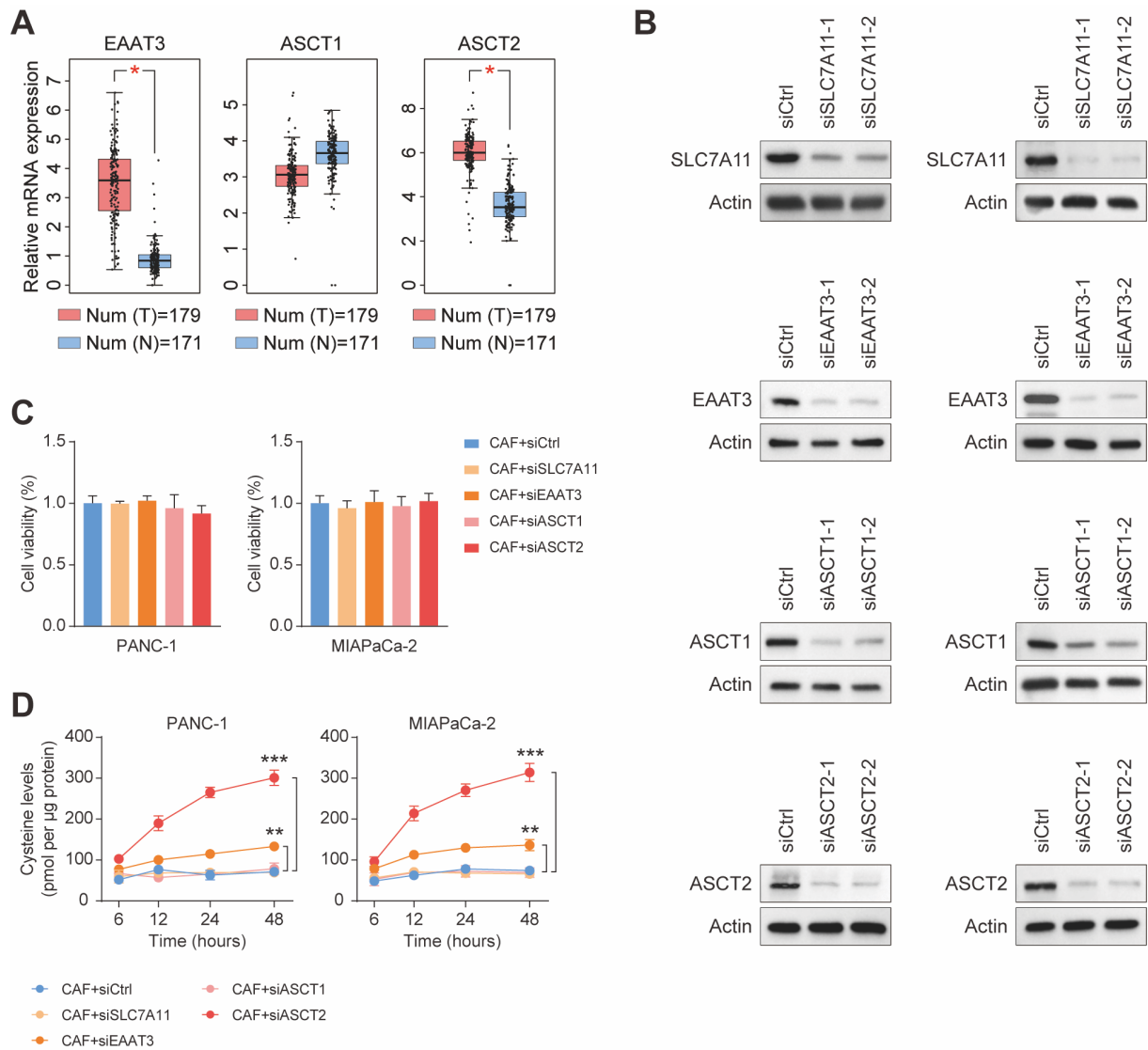
9 **Figure S2. Exocrine cysteine was essential for CAF-induced ferroptosis resistance in**  
 10 **PDAC.** (A) Cell viability was measured after treatment with CAF-CM, three repeated freeze-  
 11 thaw cycles of CAF-CM, PSC-CM, or three repeated freeze-thaw cycles of PSC-CM using  
 12 Erastin. (B) Cell viability after culture of PANC-1 cells with cysteine, angelic acid, creatine, or  
 13 glutamine, measured by CCK-8 assays. The MIAPaCa-2 cell line was cultured with Ctrl or  
 14 cysteine and treated with Erastin, (C) clonal formation assay to assess cell colony formation  
 15 capacity, and (D-E) Cell death assay to evaluate the cell death ratio of PANC-1 and MIAPaCa-  
 16 2 cells. (F) Representative IHC staining of Ki67 in mouse xenograft tumors. Scale bar = 100  
 17 microns. \*  $P < 0.05$ , \*\*  $P < 0.01$ , \*\*\*  $P < 0.001$ .

18



19

20 **Figure S3. Stromal CBS-dependent de novo biosynthesis of cysteine is required for**  
 21 **ferroptosis resistance in PDAC.** (A) After treatment of PANC-1 and MIAPaCa-2 with Ctrl,  
 22 AOAA-1, or AOAA-2, CCK-8 assays were used to measure cell viability. MIAPaCa-2 cells  
 23 were treated with shRNA or AOAA using Erastin or IKE, (B-C) CCK-8 assays were used to  
 24 measure cell viability. (D-E) EdU assays were used to measure proliferation. (F-G) colony  
 25 formation assays. (H) Images and tumor volumes of xenograft tumors (N=6). (I) Representative  
 26 H&E staining of mouse xenograft tumors and IHC staining of Ki67 and 4HNE. \*\* P < 0.01,  
 27 \*\*\* P < 0.001.



28

29

30

31

32

33

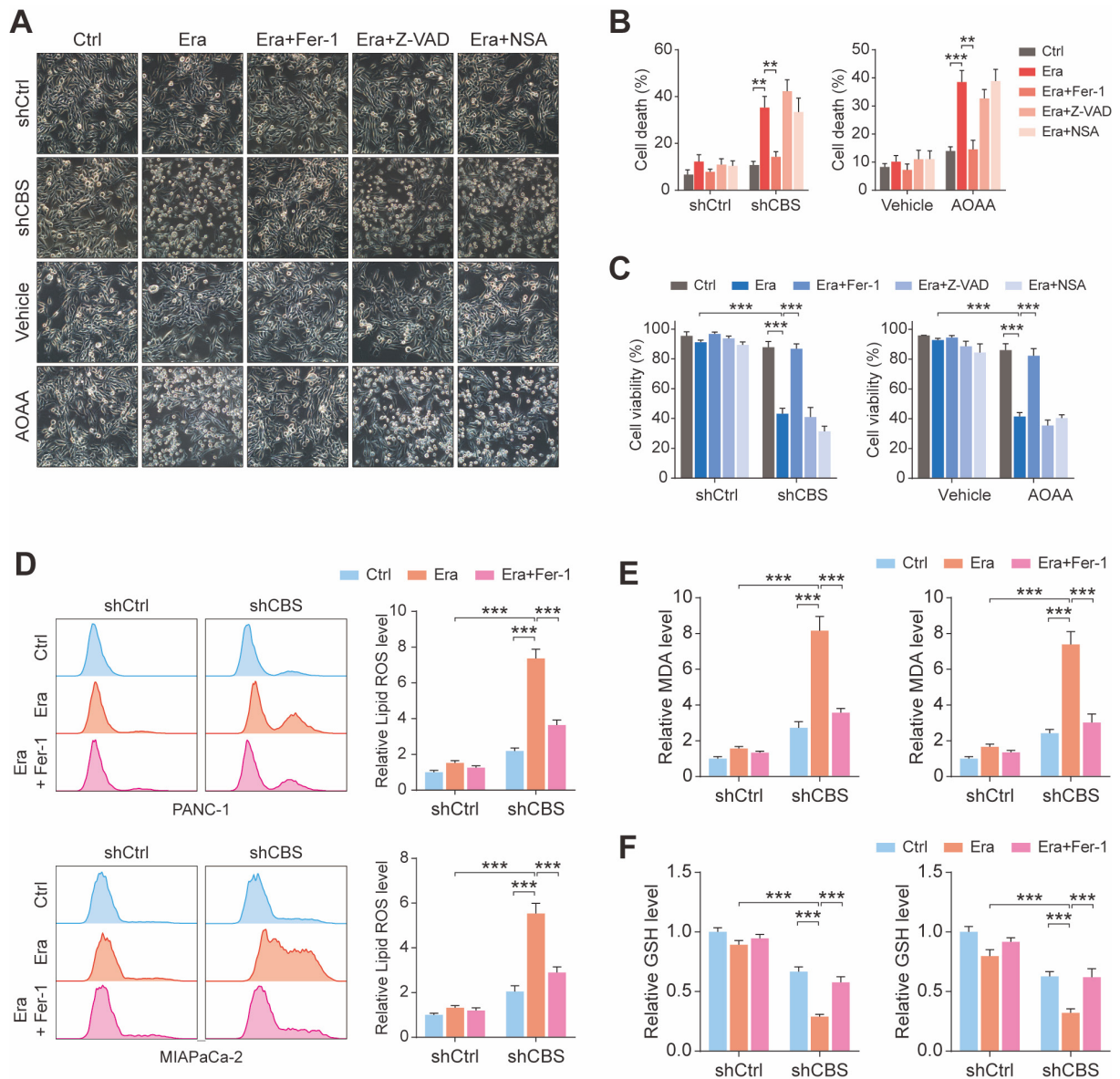
34

35

36

**Figure S4. The knockout of ASCT2 significantly impairs the uptake of cysteine by tumors.** (A) TCGA database mining of EAAT3, ASCT1, ASCT2 expression in tumor and paracancerous tissues. (B) Expression of SLC7A11, EAAT3, ASCT1 and ASCT2 knockdown efficiency of the siRNAs in cells shown by western blotting. (C) Cell viability in PANC-1 and MIAPaCa-2 cells was measured by CCK-8 assays with siSLC7A11, siEAAT3, siASCT1 or siASCT2. (D) Cysteine levels in PANC-1 and MIAPaCa-2 cells with siSLC7A11, siEAAT3, siASCT1 or siASCT2. \*  $P < 0.05$ , \*\*\*  $P < 0.001$ .





37

38 **Figure S5. Pancreatic cancer cells require exogenous cysteine-dependent GSH synthesis**

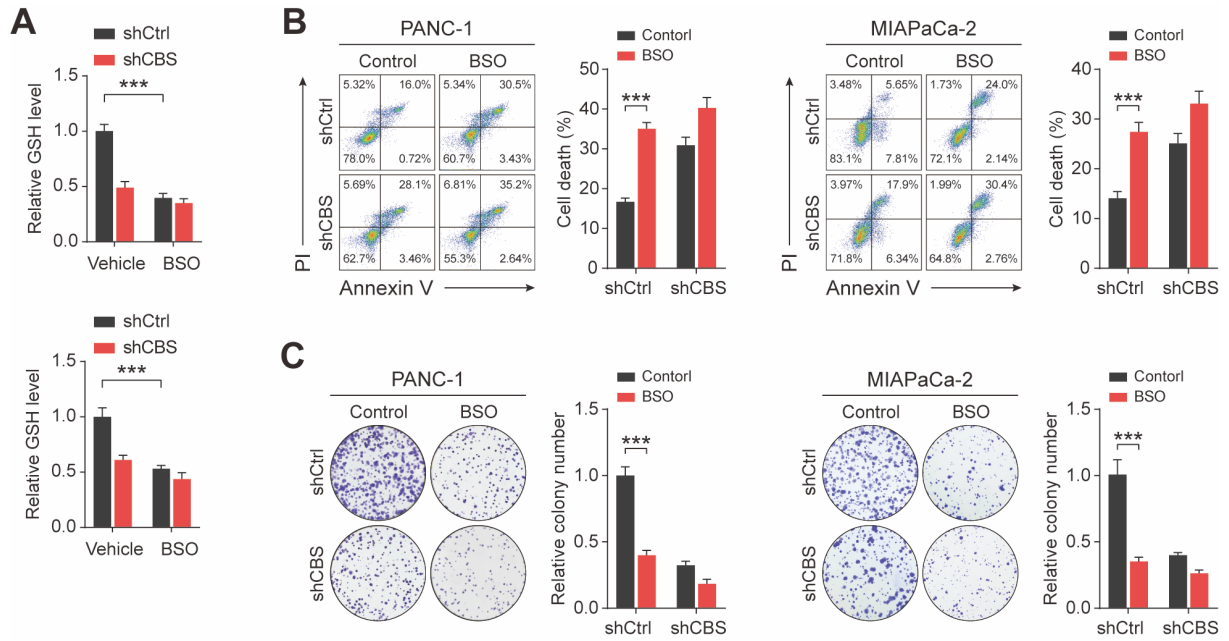
39 **to avert ferroptosis.** (A-B) Micrographs of cell death after drug treatment. (C) Flow cytometry

40 and CCK-8 assays were used to measure cell death and cell viability, respectively. (D) ROS

41 levels, assessed by flow cytometry. (E) MDA contents. (F) GSH levels. T, tumor tissue; N,

42 paracancerous tissue. \*  $P < 0.05$ , \*\*  $P < 0.01$ , \*\*\*  $P < 0.001$ .

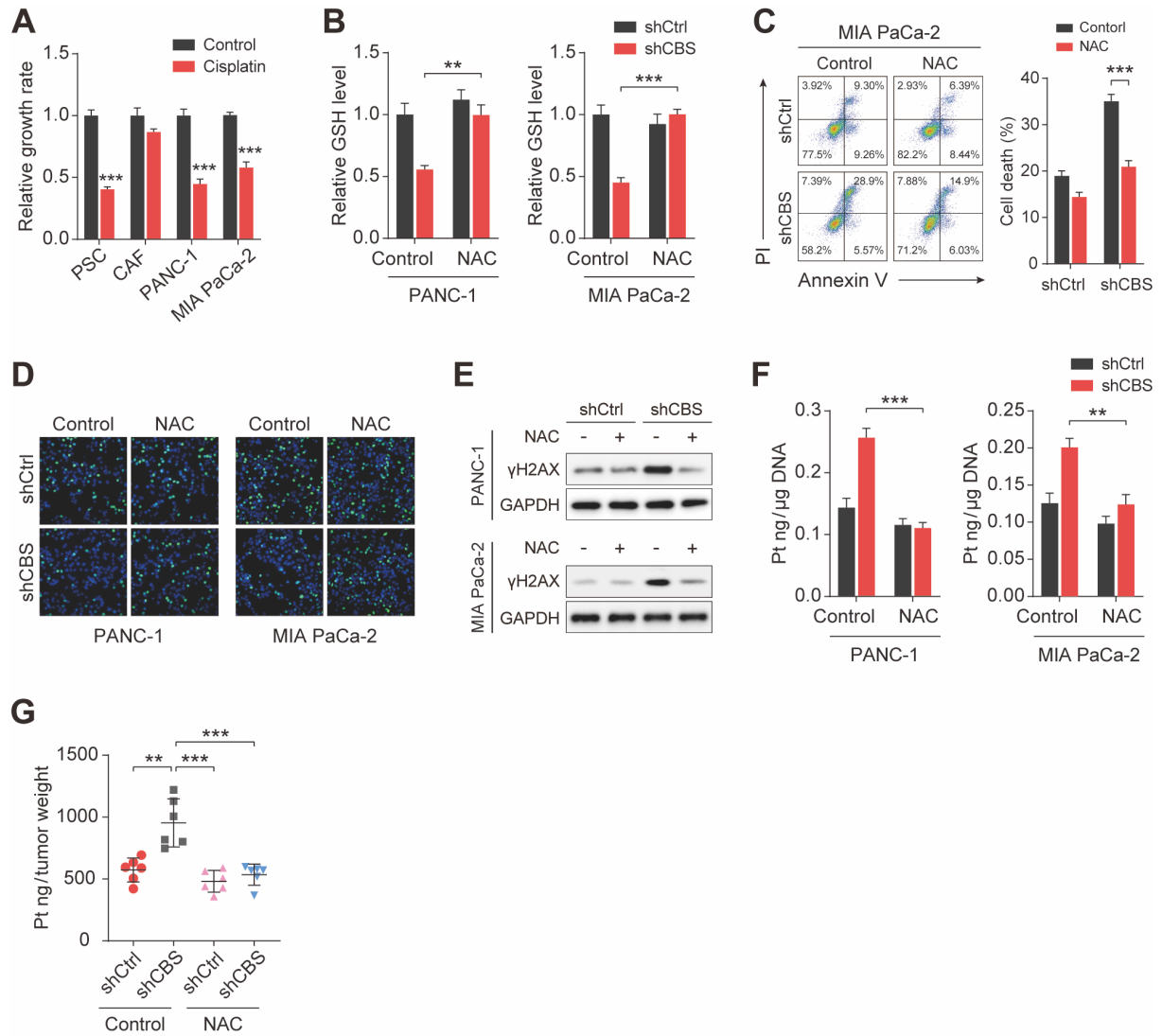
43



44

45 **Figure S6. GCLC inhibitor (BSO) decreased intracellular GSH level.** (A) GSH levels. (B)  
 46 Cell death measured by flow cytometry with BSO treatment. (C) colony formation assays with  
 47 BSO treatment. \*\*\* P < 0.001.

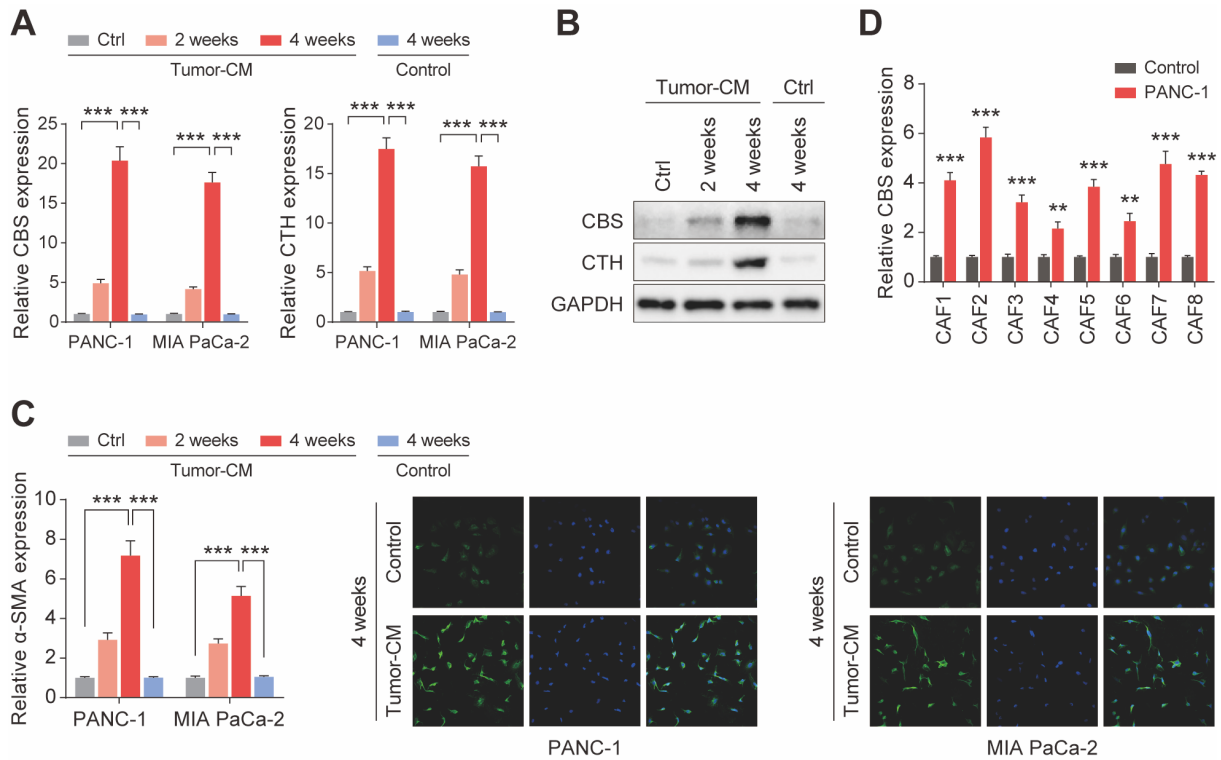
48



49

50 **Figure S7. CAFs release cysteine inducing cisplatin resistance in PDAC.** (A) Cell viability  
 51 measured by CCK-8 assays. (B) GSH levels. (C) Cell death measured by flow cytometry. (D)  
 52 Proliferation measured by EdU assays. (E) Expression of  $\gamma$ H2AX in cells shown by western  
 53 blotting. (F) ICP-MS measurement of intracellular cisplatin content. (G) Statistics on the ratio  
 54 of cisplatin content to tumor size in tumor tissue. \*\* P < 0.01, \*\*\* P < 0.001.

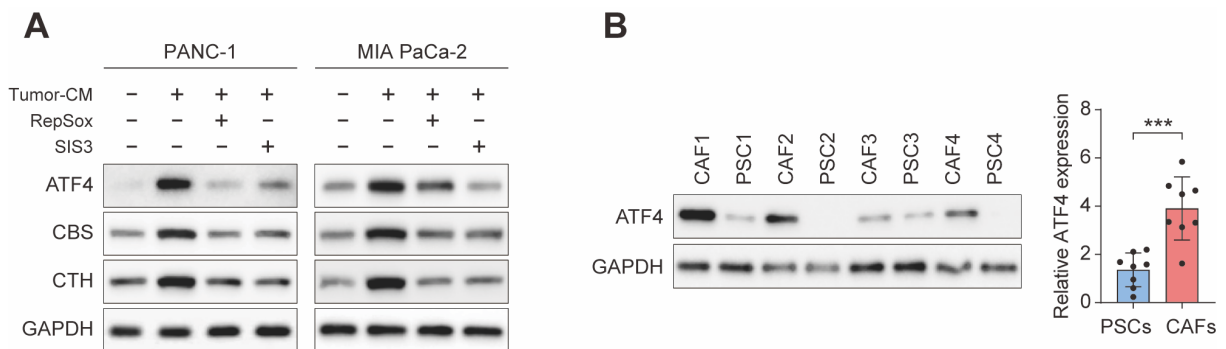
55



56

57 **Figure S8. Stromal transsulfuration pathway is regulated by TGF-β/SMAD3/ATF4**  
 58 **signaling.** (A) Expression of CBS and CTH in cells shown by RT-PCR. (B) Expression of CBS  
 59 and CTH in cells shown by western blotting. (C) Expression of α-SMA shown by RT-PCR and  
 60 immunofluorescence. (D) Expression of CBS in cells after PDAC-CM treatment shown by RT-  
 61 PCR. \*\* P < 0.01, \*\*\* P < 0.001.

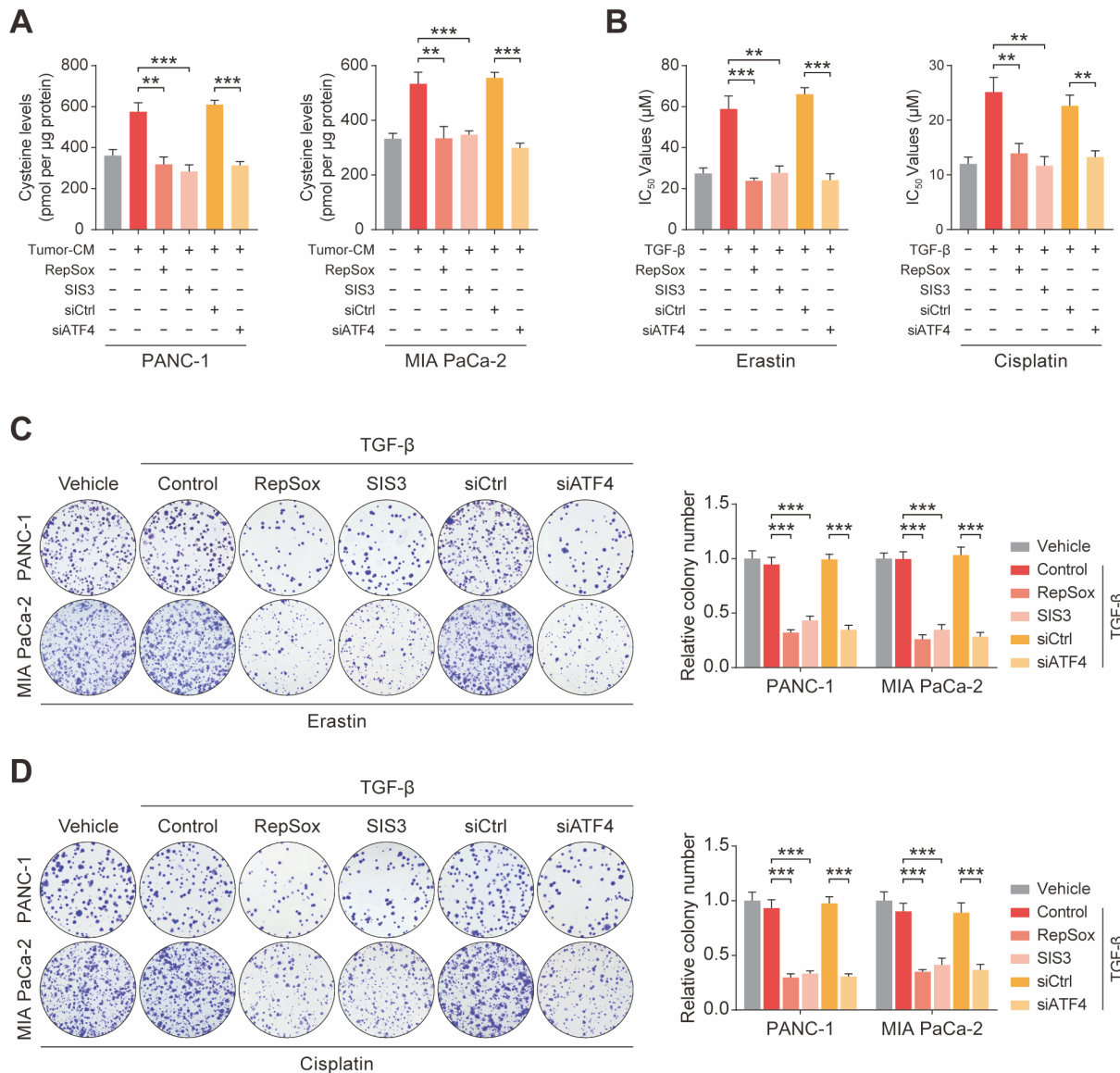
62



63

64 **Figure S9. ATF4 were significantly increased in CAFs.** (A) Expression of ATF4, CBS, and  
 65 CTH after TGF-β and RepSox antagonist treatment shown by western blotting. (B) Expression of  
 66 ATF4 in cells shown by western blotting and RT-PCR. \*\*\* P < 0.001.





67

68 **Figure S10. TGF-β/SMAD3/ATF4 signaling pathway promotes ferroptosis and cisplatin**  
 69 **resistance in PDAC.** (A) Cysteine secretion measured after inhibition of the TGF-  
 70 β/SMAD3/ATF4 signaling pathway. (B) Cell viability after treatment with different drugs,  
 71 measured by CCK-8 assays. (C-D) Colony formation by cells after treatment with Erastin or  
 72 Cisplatin. \*\* P < 0.01, \*\*\* P < 0.001.

73

**Table S1** Primer sequences.

Name	Forward primer (5' to 3')	Reverse primer (5' to 3')
CBS	ACAGAGCTCACACTTCA GGC	GGTCTGGAGACCGCTGTAAG
CTH	GCATGGGGGTACTTGACA CA	TGCACTTTGACTGAGCTCCC
SLC7A11	AAAGCCTGTTGTGTCCAC CA	AGAAAATCTGGATCCGGGCG
$\alpha$ -SMA	AGCGTGGCTATTCCTCCG TT	GCAGTGGCCATCTCATTTC
ATF4	TCGTCCTGGTGGGATCTA GG	TCTGGCATGGTTTCCAGGTC
$\beta$ -actin	AGCGAGCATCCCCAAA GTT	GGGCACGAAGGCTCATCATT